Polarization-state evolution in recirculating loops with polarization-dependent loss

Brian S. Marks, Yu Sun, Curtis R. Menyuk, and Gary M. Carter

Department of Computer Science and Electrical Engineering, University of Maryland Baltimore County, TRC 201C, 1000 Hilltop Circle, Baltimore, Maryland 21250

Received May 29, 2002

We analyze the evolution of the polarization state of a signal in a recirculating loop with polarization-dependent loss. We show that the polarization-state evolution in experiments is in qualitative agreement with our analysis, and we discuss the relationship between the polarization-state evolution and the Q factor. © 2002 Optical Society of America

OCIS codes: 260.5430, 060.2330.

Fiber recirculating loops have been extensively used as a relatively inexpensive way to study the accumulation of chromatic dispersion and nonlinearity and their interaction with other physical phenomena in long-haul transmission systems. Whereas loops have often been successful predictors of the behavior of straight-line systems with comparable parameters, it has been known for some time that, because of the periodicity of the system, the behavior of polarization phenomena in a loop can be quite different from that in a comparable straight line system. For example, it has been demonstrated that, when polarization controllers in a loop are properly set, polarization-dependent loss (PDL) can lead to the polarization of noise and to the elimination of noise that is orthogonal to the signal.[1] To break the periodicity, loop-synchronous polarization scrambling has been used to emulate more closely the polarization behavior of straight-line systems.[2] So far, most research reported in the literature has focused on the difference in performance between recirculating loops and straight-line systems. In this Letter we explain this difference by performing an analysis of the evolution of the polarization state of a signal in loops and comparing the results with those of simulations and experiments.

We have experimentally characterized the polarization behavior of our recirculating loop, which consists of 100 km of dispersion-shifted fiber compensated by 7 km of standard single-mode fiber, in which we propagate a 10-Gbit/s single-channel dispersion-managed soliton signal.[3,4] To understand the evolution of the polarization state of the signal and its effect on performance, we vary three polarization controllers—one at the input and two in the loop.[1] Once the three polarization controllers have been set to optimize the performance of the system, we systematically vary the orientation of one of the in-loop polarization controllers and collect values of the Q factor at 5000 km. Although the specific shape of the resultant Q distribution depends on the particular type of fiber used, in general we find that here the shape is more spread out and includes higher values than is the case in straight-line systems with comparable parameters and that it is often double-humped.[1] We have also reproduced this behavior in simulations. In both simulations and experiments we measured the polarization state once per round trip of the loop. For trials from the upper end of the Q distribution, the polarization state on the Poincaré sphere spirals inward to a point and converges quickly. Trials from the lower end of the distribution exhibit outward spirals that can converge on the opposite side of the Poincaré sphere. Trials from the central portion of the distribution show nearly circular evolution on the sphere, which converges slowly if at all. Each type of behavior is explained in the analysis presented here.

In our system signal degradation comes principally from noise buildup and not from pulse distortion due to polarization mode dispersion (PMD), because the PMD is very small. Therefore, we model our system by using a polarization rotation followed by a PDL element.

Because a recirculating loop system is inherently periodic, we may write its Jones transfer matrix after n round trips as $\mathbf{T} = \mathbf{M}_{\text{loop}}{}^{n}$, where $\mathbf{M}_{\text{loop}}$ is the general Jones matrix for one round trip of the loop, including polarization rotation and PDL. This 2×2 Jones matrix has a pair of complex eigenvectors $\mathbf{u}_{\pm}$ and corresponding eigenvalues $\lambda_{\pm}$. An eigenvector of $\mathbf{M}_{\text{loop}}$ is also an eigenvector of $\mathbf{T}$, and, if λ is an eigenvalue of $\mathbf{M}_{\text{loop}}$, then λ^n is an eigenvalue of $\mathbf{T}$. It follows that, if our input is an arbitrary field of the form

$$\mathbf{u}_{\text{in}} = c_{+}\mathbf{u}_{+} + c_{-}\mathbf{u}_{-}, \tag{1}$$

then the output field vector is

$$\mathbf{u}_{\text{out}} = \mathbf{T}\mathbf{u}_{\text{in}} = c_{+}\lambda_{+}{}^{n}\mathbf{u}_{+} + c_{-}\lambda_{-}{}^{n}\mathbf{u}_{-}. \tag{2}$$

If we let $\lambda_{\pm} = |\lambda_{\pm}|\exp(i\phi_{\pm})$ and $c_{\pm} = |c_{\pm}|\exp(i\psi_{\pm})$, then the corresponding output Stokes vector is $\mathbf{s}_{\text{out}} = (\mathbf{u}_{\text{out}}{}^{\dagger}\sigma_3\mathbf{u}_{\text{out}}, \mathbf{u}_{\text{out}}{}^{\dagger}\sigma_1\mathbf{u}_{\text{out}}, -\mathbf{u}_{\text{out}}{}^{\dagger}\sigma_2\mathbf{u}_{\text{out}})^{T}$, yielding

$$\mathbf{s}_{\text{out}} = |c_{+}|^2|\lambda_{+}|^{2n}\mathbf{s}_{+} + |c_{-}|^2|\lambda_{-}|^{2n}\mathbf{s}_{-} + 2|c_{+}||c_{-}|(|\lambda_{+}||\lambda_{-}|)^{n}\text{Re}\{\mathbf{s}_{c}\exp[-i(n\Delta\phi + \Delta\psi)]\}, \tag{3}$$

where $\mathbf{s}_{\pm} \equiv (\mathbf{u}_{\pm}{}^{\dagger}\sigma_3\mathbf{u}_{\pm}, \mathbf{u}_{\pm}{}^{\dagger}\sigma_1\mathbf{u}_{\pm}, -\mathbf{u}_{\pm}{}^{\dagger}\sigma_2\mathbf{u}_{\pm})^{T}$, $\mathbf{s}_{c} \equiv (\mathbf{u}_{+}{}^{\dagger}\sigma_3\mathbf{u}_{-}, \mathbf{u}_{\pm}{}^{\dagger}\sigma_1\mathbf{u}_{-}, -\mathbf{u}_{+}{}^{\dagger}\sigma_2\mathbf{u}_{-})^{T}$, $\Delta\phi \equiv \phi_{+} - \phi_{-}$, and $\Delta\psi \equiv \psi_{+} - \psi_{-}$. In the above expressions, σ_k represent the standard Pauli spin matrices. In Eq. (3), if the eigenvalues have different magnitudes, then

0146-9592/02/211881-03$15.00/0

one obtains spiral motion. The spiral centers are given by one of the polarization eigenstates, $\mathbf{s}_{\pm}$, and the rotation is described by the third term, where the rotation angle of the spiral that is due to one round trip of the recirculating loop is given by the phase difference of the eigenvalues, $\Delta\phi$. The ratio of the magnitudes of the eigenvalues gives the relative decay rate of each of the coefficients, thus yielding the rate of convergence to a spiral center.

To understand the spiral behavior in a loop with PDL we consider a transfer matrix of the form

$$\mathbf{M}_{\text{loop}} = \mathbf{M}_{\text{PDL}}\mathbf{M}_{\text{rot}}, \tag{4}$$

where $\mathbf{M}_{\text{rot}}$ is a unitary matrix representing a fixed rotation on the Poincaré sphere and $\mathbf{M}_{\text{PDL}}$ represents the effect of PDL in one round trip of the loop. Inasmuch as an arbitrary rotation on the Poincaré sphere can be expressed as a rotation through an angle 2γ about an axis given by a unit vector $\hat{\mathbf{s}}_{\text{rot}} = (x, y, z)^T$, matrix $\mathbf{M}_{\text{rot}}$ can be expressed in the form

$$\mathbf{M}_{\text{rot}} = \begin{bmatrix} \cos\gamma + ix\sin\gamma & -(z - iy)\sin\gamma \\ (z + iy)\sin\gamma & \cos\gamma - ix\sin\gamma \end{bmatrix}. \tag{5}$$

The effect of PDL is modeled by the Jones matrix

$$\mathbf{M}_{\text{PDL}} = \begin{bmatrix} 1 & 0 \\ 0 & 1 - \epsilon \end{bmatrix}. \tag{6}$$

where the strength of the PDL is given by a small nonnegative parameter ϵ that is less than 1. Note that, in this notation, the low-loss axis of the PDL is given by $\hat{\mathbf{s}}_{\text{PDL}} = (1, 0, 0)^T$ in Stokes space.

We exploit the fact that ϵ is small by using standard perturbation methods to expand our eigenvector in powers of ϵ, solving for corrections at each order.[5] We begin by seeking eigenvalues and eigenvectors that satisfy $(\mathbf{M}_{\text{loop}} - \lambda\mathbf{I})\mathbf{u} = 0$, where $\mathbf{I}$ is the 2×2 identity matrix, and expand λ and $\mathbf{u}$ in power series in ϵ as $\lambda_{\pm} = \lambda_0 + \epsilon\lambda_1 + O(\epsilon^2)$ and $\mathbf{u}_{\pm} = \mathbf{u}_0 + \epsilon\mathbf{u}_1 + O(\epsilon^2)$. From these expressions we can compute the Stokes eigenvector in powers of ϵ as well, obtaining $\mathbf{s}_{\pm} = \mathbf{s}_{\pm}^{(0)} + \epsilon\mathbf{s}_{\pm}^{(1)} + O(\epsilon^2)$. The $O(1)$ problem $(\mathbf{M}_{\text{rot}} - \lambda_0\mathbf{I})\mathbf{u}_0 = \mathbf{0}$, which we obtain by setting $\epsilon = 0$, corresponds to a rotation when the effect of PDL is neglected. The leading-order eigenvalues are $\lambda_0 = \exp(\pm i\gamma)$, and the leading-order eigenvectors are

$$\mathbf{u}_0 = (2 \mp 2x)^{-1/2}\begin{bmatrix} z - iy \\ i(x \mp 1) \end{bmatrix}, \tag{7}$$

where we have normalized these eigenvectors such that they have unit length. It is straightforward then to show that these eigenvectors in Jones space yield the corresponding Stokes vectors $\mathbf{s}_{\pm}^{(0)} = \pm\hat{\mathbf{s}}_{\text{rot}}$, as expected in the $O(1)$ problem.

The $O(\epsilon)$ eigenvalue correction is given by $\lambda_1 = -\frac{1}{2}(1 \mp x)\exp(\pm i\gamma)$. Similarly, the $O(\epsilon)$ correction to the eigenvector satisfies the generalized eigenvector equation

$$(\mathbf{M}_{\text{rot}} - \lambda_0\mathbf{I})\mathbf{u}_1 = \left\{\begin{bmatrix} 0 & 0 \\ 0 & 1 \end{bmatrix}\mathbf{M}_{\text{rot}} + \lambda_1\mathbf{I}\right\}\mathbf{u}_0, \tag{8}$$

which yields

$$\begin{aligned}\mathbf{u}_1 &= ik\mathbf{u}_0 + \mathbf{u}_1' \\ &\equiv ik\mathbf{u}_0 + \frac{\csc\gamma}{2\sqrt{2}}\exp(\pm i\gamma)\sqrt{1 \mp x}\begin{pmatrix} 0 \\ 1 \end{pmatrix},\end{aligned} \tag{9}$$

where k is a real constant whose value is not determined until the $O(\epsilon^2)$ level. The $O(\epsilon)$ correction to the eigenvector in Stokes space is then given by

$$\mathbf{s}_{\pm}^{(1)} = 2\,\text{Re}\begin{pmatrix} \mathbf{u}_0^{\dagger}\sigma_3\mathbf{u}_1' \\ \mathbf{u}_0^{\dagger}\sigma_1\mathbf{u}_1' \\ -\mathbf{u}_0^{\dagger}\sigma_2\mathbf{u}_1' \end{pmatrix} = \frac{1}{2}\begin{pmatrix} 1 \mp x \\ z\cot\gamma \mp y \\ -y\cot\gamma \pm z \end{pmatrix}. \tag{10}$$

To $O(\epsilon)$, we may concisely write the Stokes eigenvectors as

$$\begin{aligned}\mathbf{s}_{\pm} = \pm\,\hat{\mathbf{s}}_{\text{rot}} + {}&{}^1\!/_2\,\epsilon[\hat{\mathbf{s}}_{\text{PDL}} \mp \hat{\mathbf{s}}_{\text{rot}} \\ &+ (\hat{\mathbf{s}}_{\text{rot}} \times \hat{\mathbf{s}}_{\text{PDL}})\cot\gamma] + O(\epsilon^2).\end{aligned} \tag{11}$$

Note that, because of the $O(\epsilon)$ corrections, the eigenstates in Stokes space are not antiparallel in the presence of PDL, unlike the principal states for PMD.[6]

To obtain the explicit form of the output Stokes vector in the loop model we still need expressions for $|\lambda_{\pm}|$ and $\mathbf{s}_c$. We use the asymptotic expansion; the coefficients in Eq. (3) are given by $A_{\pm} \equiv |\lambda_{\pm}|^2 = 1 - \epsilon(1 \mp x) + O(\epsilon^2)$ and $B \equiv |\lambda_+||\lambda_-| = 1 - \epsilon + O(\epsilon^2)$. As $A_{\pm}$ and B are less than 1, $A_{\pm}^n$ and B^n decay as $n \to \infty$. The slowest-decaying term of the three terms in Eq. (3) is the dominant term, which determines the attracting eigenstate. The relative decay rate of each of the terms in Eq. (3) is determined by the inequalities $A_+ \gtrless B \gtrless A_-$, which hold when $x \gtrless 0$. Thus, if the low-loss axis of the PDL $\hat{\mathbf{s}}_{\text{PDL}}$ is in the same hemisphere as rotation axis $\hat{\mathbf{s}}_{\text{rot}}$, then the $\mathbf{s}_+$ eigenstate is the attracting eigenstate. The converse is also true. We conclude that, if $x \neq 0$, we have spiral motion toward one of the eigenstates but, if $x = 0$, all terms remain comparable and we observe nearly circular behavior on the Poincaré sphere. From the expressions for λ_0 and λ_1 it follows that

$$\exp(i\phi_{\pm}) = \lambda_{\pm}/|\lambda_{\pm}| = \exp(\pm i\gamma) + O(\epsilon^2), \tag{12}$$

so that, to $O(\epsilon^2)$, $\Delta\phi = 2\gamma$. We also obtain

$$\mathbf{s}_c = (i\hat{\mathbf{t}}_1 - \hat{\mathbf{t}}_2)[1 - (\epsilon/2)(1 + i\cot\gamma)] + O(\epsilon^2), \tag{13}$$

where $\hat{\mathbf{t}}_1 \equiv (\hat{\mathbf{s}}_{\text{rot}} \times \hat{\mathbf{s}}_{\text{PDL}})/|\hat{\mathbf{s}}_{\text{rot}} \times \hat{\mathbf{s}}_{\text{PDL}}|$ and $\hat{\mathbf{t}}_2 \equiv [\hat{\mathbf{s}}_{\text{rot}} \times (\hat{\mathbf{s}}_{\text{rot}} \times \hat{\mathbf{s}}_{\text{PDL}})]/|\hat{\mathbf{s}}_{\text{rot}} \times \hat{\mathbf{s}}_{\text{PDL}}|$. Therefore the output Stokes vector is

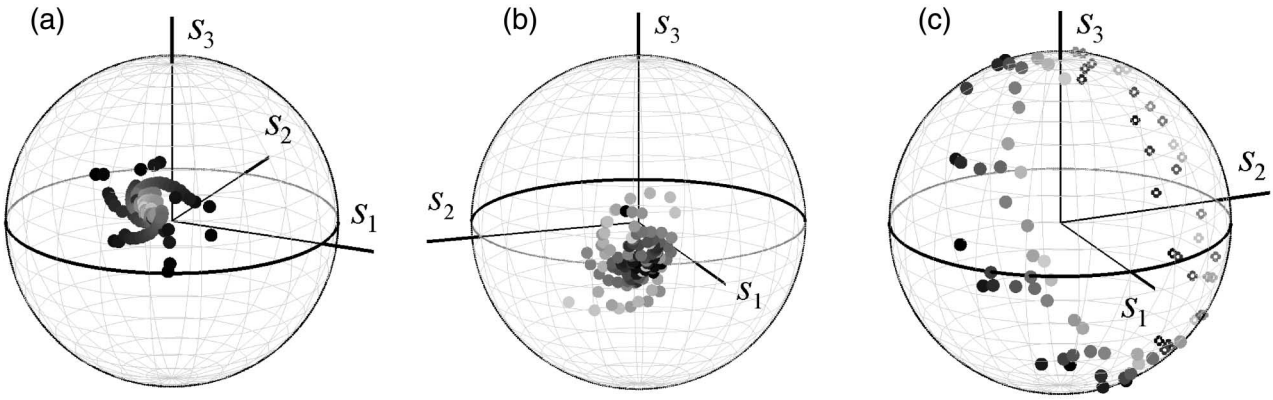

Fig. 1. Experimentally measured evolution of the polarization state on the Poincaré sphere, showing spiral behavior that corresponds to (a) a high Q value with a spiral inward, (b) a low Q value with an outgoing spiral, and (c) a medium Q value with a nearly circular trajectory around the sphere. The gray scale denotes transmission distance, where dark to light indicates increasing propagation distance.

$$\begin{aligned}\mathbf{s}_{\text{out}} = {} & A_+{}^n|c_+|^2\mathbf{s}_+ + A_-{}^n|c_-|^2\mathbf{s}_- \\ & + 2B^n|c_+||c_-|(\hat{\mathbf{t}}_1 \sin\zeta_n - \hat{\mathbf{t}}_2\cos\zeta_n \\ & + (\epsilon/2)\{\hat{\mathbf{t}}_1[\cot\gamma\cos\zeta_n - \sin\zeta_n] \\ & + \hat{\mathbf{t}}_2[\cos\zeta_n + \cot\gamma\sin\zeta_n]\}) + O(\epsilon^2), \qquad (14)\end{aligned}$$

where $\zeta_n \equiv 2n\gamma + \Delta\psi$.

Neglecting the ϵ contributions in Eq. (14), we note that the B^n term contains sinusoidal pieces that correspond to the spiral or circular motion on the Poincaré sphere. We compare the spiral behavior from the experimental results shown in Fig. 1 with the analytical result in Eq. (14). In Eq. (14) we have an inward spiral evolution if $A_\pm > B > A_\mp$ and the input polarization state is closer to the attracting $\mathbf{s}_\pm$ eigenstates, i.e., $|c_\pm| > |c_\mp|$, so the signal's polarization state remains on the same hemisphere as the low-loss axis of the PDL throughout transmission, corresponding to high Q. This situation is illustrated in Fig. 1(a), in which the center of the spiral is the attracting eigenstate. Conversely, we have an outward spiral if $A_\pm > B > A_\mp$ and the input polarization state is close to the repelling $\mathbf{s}_\mp$ eigenstate, i.e., $|c_\pm| < |c_\mp|$. In this case the signal's polarization state can remain for a long time on the same hemisphere as the high-loss axis of the PDL, particularly if $|c_\pm| \ll |c_\mp|$, corresponding to a low Q. This situation corresponds to Fig. 1(b), in which the center of the spiral is the repelling eigenstate. Finally, if $A_+ \approx B \approx A_-$, then there is a slow convergence because no single term dominates. In this case the circle's center is orthogonal to the low-loss axis of the PDL, and the signal passes alternately through the high-loss and low-loss axes of the PDL, corresponding to a medium Q. This situation corresponds to the polarization evolution shown in Fig. 1(c), in which there seems to be no attracting or repelling state.

The experimental and theoretical results show that PDL plays a major role in the loop performance and polarization-state evolution. In recirculating loop systems, the PDL will unrealistically improve the performance when the polarization evolution is optimized by use of a polarization controller. The noise tends to polarize in the polarization state of the signal, and the noise that is orthogonal to the signal is reduced.[1] We have characterized the behavior of the polarization state as a spiral evolution on the Poincaré sphere and have associated different types of spiral with different system performance.

The authors acknowledge support from the National Science Foundation and the U.S. Department of Energy. The authors are grateful to Ivan Lima for useful discussions and to Kevin Allen for helping us with the figures. B. Marks and G. Carter also acknowledge support from the Laboratory for Physical Sciences, College Park, Md. B. S. Marks' e-mail address is marks@umbc.edu.

References

1. Y. Sun, I. T. Lima, Jr., H. Jiao, J. Wen, H. Xu, H. Ereifej, G. M. Carter, and C. R. Menyuk, IEEE Photon. Technol. Lett. **13,** 966 (2001).
2. S. Lee, Q. Yu, L.-S. Yan, Y. Xie, O. H. Adamczyk, and A. E. Willner, in *Optical Fiber Communication Conference (OFC)*, Vol. 54 of OSA Trends in Optics and Photonics Series (Optical Society of America, Washington, D.C., 2001), paper WT2 (2001).
3. G. M. Carter, R.-M. Mu, V. S. Grigoryan, C. R. Menyuk, P. Sinha, T. F. Carruthers, M. L. Dennis, and I. N. Dulling III, Electron. Lett. **35,** 233 (1999).
4. Y. Sun, B. S. Marks, I. T. Lima, Jr., K. Allen, G. M. Carter, and C. R. Menyuk, in *Optical Fiber Communication Conference*, Vol. 70 of OSA Trends in Optics and Photonics Series (Optical Society of America, Washington, D.C., 2002), paper ThI4.
5. J. Kevorkian and J. D. Cole, *Multiple Scale and Singular Perturbation Methods* (Springer-Verlag, New York, 1996).
6. B. Huttner, C. Geiser, and N. Gisin, J. Sel. Top. Quantum Electron. **6,** 317 (2000).